A Deterministic Method for Generating Flame-Length Probabilities

Joe H. Scott, Principal Wildfire Analyst, Pyrologix LLC

Abstract—Wildfire risk assessments rely on flame-length probabilities—the conditional probabilities that fire intensity will be within various flame-length classes. The factors affecting flame-length probability include the elements of the fire-behavior triangle—fuel, weather, and topography—plus the orientation of the flaming front relative to the heading direction. Current methods for determining flame-length probabilities include: (1) a single deterministic simulation of flame length at the head of the fire for one weather type (wind speed, wind direction, fuel moisture content); (2) multiple deterministic simulations of flame length at the head of the fire (for several weather types), which are then integrated; and (3) stochastic simulation of fire growth and flame length across a few to several dozen weather types. In this paper, we describe a deterministic process, called FLEP-Gen, that addresses shortcomings of the current methods. It improves upon the multiple-simulation approach by (1) incorporating fire intensity in non-heading spread directions and (2) weighting the weather types by their relative area burned rather than just their temporal relative frequencies. We present the mathematical basis for the process—based on the geometry of an ellipse—as well as spatial and nonspatial examples of its application to various fire management problems.

Keywords: wildfire hazard, fire intensity, flame length, effects analysis, elliptical dimensions

INTRODUCTION AND BACKGROUND

Fire intensity is a measure of the rate of heat release at the flaming front of a spreading wildland fire (Alexander 1982). Along with burn probability (the likelihood of fire burning a given point on the landscape), fire intensity is a primary component of wildfire hazard and is the main fire-behavior characteristic influencing the effects of wildfire on resources and assets (Scott et al. 2013; Thompson et al. 2013). Fire intensity is commonly measured by Byram's fireline intensity (kW/m) or by the length of flames generated (Scott 2012). There are two simple mathematical models in operational use in the United States that relate Byram's fireline intensity (FLI) to flame length (Byram 1959; Thomas 1963). In the suite of operational spatial models developed and supported by the Missoula Fire Sciences Laboratory (FARSITE, FlamMap, FSim, etc.; visit https://www.firelab.org/applications), the Byram model is applied to all surface fires, and the Thomas model is applied to passive and active crown fires.

For use in fire management planning systems, fire intensity has been classified into six Fire Intensity Levels (FILs). Although the FIL classification is nominally based on flame length (Roose et al. 2008), the *FLI* values that correspond to the flame-length class breaks for the two flame-length models can be determined (table 1).

An effects analysis relies on the conditional probability distribution across the FILs (Finney 2005; Scott et al. 2013). For an effects analysis, one must know the conditional probability—given that a fire occurs at a location—that fire intensity will be in each of the six FILs. Because FILs are indexed by flame length,

In: Hood, Sharon; Drury, Stacy; Steelman, Toddi; Steffens, Ron, tech. eds. The fire continuum—preparing for the future of wildland fire: Proceedings of the Fire Continuum Conference. 21-24 May 2018, Missoula, MT. Proc. RMRS-P-78. Fort Collins, CO: U.S. Department of Agriculture, Forest Service, Rocky Mountain Research Station. 358 p.

Papers published in these proceedings were submitted by authors in electronic media. Editing was done for readability and to ensure consistent format and style. Authors are responsible for content and accuracy of their individual papers and the quality of illustrative materials. Opinions expressed may not necessarily reflect the position of the U.S. Department of Agriculture.

Table 1—Six Fire Intensity Levels (FILs) as defined by flame length (ft) following Roose et al. (2008). The fireline intensity values corresponding to those flame-length values are shown as well. In operational spatial fire modeling systems developed by the Missoula Fire Sciences Laboratory, the Byram (1959) flame-length model is applied to surface fires and the Thomas (1963) model is applied to passive and active crown fires.

Fire intensity level (FIL)	Flame-length range (ft)	Flame-length range (m)	Surface fireline intensity (FLI) range (kW/m)	Crown fire fireline intensity (FLI) range (kW/m)
FIL1	< 2	< 0.6	< 88.6	< 108
FIL2	2–4	0.6–1.2	88.6–400	108–303
FIL3	4–6	1.2–1.8	400–965	303–554
FIL4	6–8	1.8–2.4	965–1803	554–851
FIL5	8–12	2.4–3.7	1803–4354	851–1559
FIL6	> 12	> 3.7	> 4354	> 1559

these are called conditional flame-length probabilities (*FLP*s). The sum of *FLP*s across all FILs equals 1.

Factors affecting fire intensity include the elements of the fire-behavior triangle—fuel, weather, and topography—plus a fourth factor, relative spread direction. Relative spread direction is the orientation of the flaming front relative to the heading direction—heading, flanking, and backing spread directions, and all directions between (Finney 1998; Scott 2007, 2012). Topography and some fuel characteristics, including fuel load and arrangement, are temporally constant within a fire season. Weather-related fire-environment variables, including wind speed, wind direction, and fuel moisture content, can vary considerably within a season, from day to day, and even from hour to hour (see Scott 2012).

Current methods for assessing fire intensity for use in a spatial wildfire hazard and risk assessment include:

- Single deterministic simulation of fire intensity at the head of the fire for one weather type (wind speed, wind direction, fuel moisture content). This results in a single fire intensity value for a pixel, and that fire intensity can be classified into an FIL.
- Multiple deterministic simulations of fire intensity at the head of the fire (for several weather types), which are then integrated into a single fire intensity value for the pixel; the simulations are typically weighted by the temporal relative frequency of the weather types.
- Stochastic simulation of fire growth across a few to several dozen weather types. Rather than producing a single fire intensity value for a pixel, a stochastic simulation produces a probability distribution of fire intensity across the FILs—the conditional *FLP*s—at each pixel.

These approaches have relative advantages and disadvantages. The single-simulation approach can be run at a fine pixel size (30 m) but fails to account for two important factors affecting fire intensity: the wide variety of weather types under which a pixel can burn, and non-heading spread directions, for which fire intensity is considerably lower than at the head of the fire.

The multiple-simulation approach accounts for some variability in weather types but still focuses on the head of the fire. Current methods of weighting the weather types (weighting by temporal relative frequency) do not account for any potential differences in area burned among the weather types. For example, even though strong winds occur rarely in time, the high spread rates associated with them mean that they should account for a larger proportion of overall area burned than the temporal relative frequency alone would suggest.

The stochastic simulation approach addresses several of the shortcomings of the deterministic simulation approaches by inherently weighting the weather types and spread directions by their actual influence on the landscape. But two disadvantages remain: the stochastic simulations cannot be accomplished across a large landscape at 30-m resolution, and limitations on computing time generally result in a small sample size from which to determine the distribution of flame lengths. For example, a typical pixel will burn just 10-100 times during a 10,000-iteration FSim run, and those 10-100 instances are classified into six flame-length probability bins. That is a small sample size to determine the relative frequency of flame length in those bins, but larger sample sizes are computationally unattainable.

In this paper a deterministic process, called FLEP-Gen, that addresses shortcomings of the current methods is described. It improves upon the multiple-simulation approach by (1) incorporating fire intensity in non-heading spread directions and (2) weighting the weather types by their relative area burned in combination with their temporal relative frequency rather than just their temporal relative frequencies.

NON-HEADING INTENSITY

By assuming that a wildfire grows as an ellipse with the ignition at the rear focus (Alexander 1985), the geometric properties of an ellipse can be used to find the relative fire-area burned at or above a given *FLI* based on just two factors—the *FLI* at the head of the fire and the length-to-breadth ratio (*LB*) of the ellipse (Alexander 1982; Catchpole et al. 1992). Following Finney (1998), *LB* can be estimated as

$$LB = 0.936e^{(0.1147U_m)} + 0.461e^{-.0692U_m} - 0.397$$

where U_m is the effective midflame wind speed (mi/h) after combining (vectoring) midflame wind speed, slope steepness, and wind direction (Finney 1998).

For surface fires, midflame wind speed is a function of fuelbed depth for unsheltered fuelbeds or a function of canopy cover and canopy height for fuelbeds sheltered by a forest canopy (Albini and Baughman 1979). For passive and active crown fires, midflame wind speed (for the purposes of estimating *LB*) is taken to be half of the 20-ft wind speed (Albini and Baughman 1979; Finney 1998). The backing ratio (*BR*), the ratio of backing spread rate to heading spread rate, can be calculated from *LB* as

$$BR = \frac{LB - \sqrt{LB^2 - 1}}{LB + \sqrt{LB^2 - 1}}$$

Certain elliptical dimensions (fig. 1) can be calculated from the headfire rate of spread (ROS_{head}), *LB*, and *BR* following equations taken directly or modified from Catchpole et al. (1992) and Finney (1998). The labeling of the elliptical dimensions *a* and *b* are reversed in Finney (1998) compared to Catchpole et al. (1992); this paper uses the labeling of Catchpole et al. (1992), for which the parameter *a* is the half-length of the ellipse length and *b* is the half-width:

$$a = \frac{ROS_{head}(1 + BR)}{2}$$

$$b = \frac{a}{LB}$$

$$c = a\sqrt{1 - LB^{-2}}$$

Following Catchpole et al. (1992), the proportional *FLI* (or *ROS*) can be determined for a given angle θ as a function of elliptical dimensions defined above:

$$PropFLI_{\emptyset} = \frac{\dfrac{b(a + c\cos\emptyset)}{\sqrt{a^2\sin^2\emptyset + b^2\cos^2\emptyset}}}{a + c}$$

where θ is the angle of the subtending circle of the ellipse (Catchpole et al. 1992). The proportional fire-area burned at or above that proportional *FLI* can be determined for the same angle θ as:

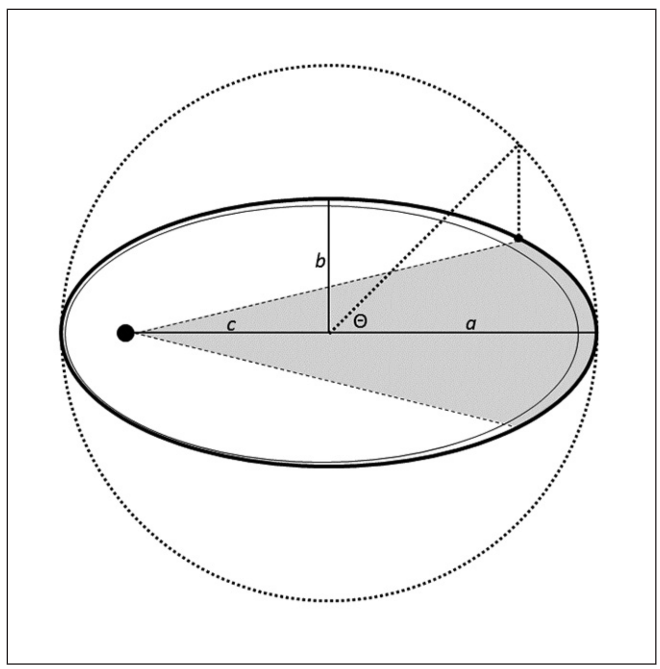

Figure 1—Elliptical dimensions *a*, *b*, and *c* as defined by Catchpole et al. (1992), where the angle Θ identifies a point on the ellipse based on the subtending circle, shown as the dotted circle. The shaded area represents the proportional fire-area burned at or above the proportional fireline intensity for a given Θ.

$$PropArea_{\emptyset} = \frac{(a\emptyset + c\sin\emptyset)}{\pi a}$$

The proportional area burned above any proportional intensity can then be plotted for a range of θ and for a range of *LB* values (fig. 2). This permits one to find the proportional fire-area burned at or above a given proportional fireline intensity value.

To use these equations operationally, the required proportional *FLI* is calculated as the ratio of threshold *FLI* for a given FIL class break (table 1) to the headfire *FLI*. Knowledge of the elliptical dimensions permits brute-force estimation (by iteration) of the subtending angle θ that produces the required proportional *FLI*; from θ, one can then calculate the proportional fire-area burned at or above the threshold *FLI*. This proportional fire-area burned is taken to be the probability of exceeding the threshold flame-length value, also called the flame-length exceedance probabilities (*FLEP*s) for the FIL class breaks. The *FLP*s are calculated from the *FLEP*s by subtraction. For example, the probability that flame length will be in FIL2 (flame lengths between 2 and 4 ft) is the probability of FL exceeding 2 ft minus the probability of FL exceeding 4 ft.

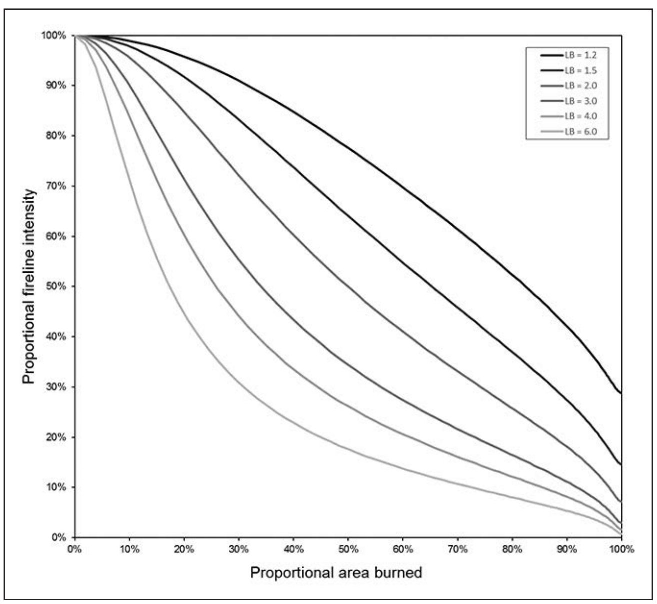

Figure 2—Plot of proportional fireline intensity against proportional fire-area burned for a range of length-to-breadth ratios. This figure is analogous to figure 4 of Catchpole et al. (1992).

The estimation of *FLP*s using this process can be illustrated for a simple fire environment of heavy shrub fuel (fuel model SH5; Scott and Burgan 2005) on flat ground under a 15 mi/h wind speed at the 6.1-m (20-ft) height. The example assumes dead fuel moisture contents of 4 percent for the 1-h timelag class, 5 percent for 10-h and 6 percent for 100-h, and 110 percent for the moisture content of live the woody component. Using Rothermel's (1972) surface fire-spread model as implemented in Nexus (Scott and Reinhardt 2001), the headfire intensity is 9,770 kW/m (*FL* = 17.4 ft). For that headfire intensity one can estimate the required proportional intensity values that correspond to the flame-length breakpoints, and then the proportional areas that correspond to those proportional intensities (table 2, fig. 3). These proportional areas represent the relative proportion of burned area exceeding the upper end of the flame-length range for each FIL. In this example, 49.87 percent of the elliptical fire area is burned at or above the 12-ft flame-length threshold (4,354 kW/m), 85.68 percent of the area is burned above an 8-ft flame-length threshold, 96.22 percent above a flame length of 6 ft, and 100 percent above 4 ft (table 2). The minimum fireline intensity, corresponding to the rear of the fire, is greater than the threshold for a 4-ft flame length, so 100 percent of the fire area would burn above this threshold. By subtraction, 0 percent of the fire area is burned in FIL1 and FIL2, 3.78 percent in FIL3, 10.54 percent in FIL4, 35.81 percent in FIL5, and 49.87 percent in FIL6. Note that the sum of these FLPs is 100 percent.

Table 2—Proportional intensity and proportional area burned for FIL class breaks, for a headfire fireline intensity = 9,770 kW/m and LB ratio = 2.275.

Fire intensity level	Proportional intensity	Proportional area (FLEP)
2' (FIL1/2)	0.00907	1.0000
4' (FIL2/3)	0.04091	1.0000
6' (FIL3/4)	0.09876	0.9622
8' (FIL4/5)	0.18459	0.8568
12' (FIL5/6)	0.44566	0.4987

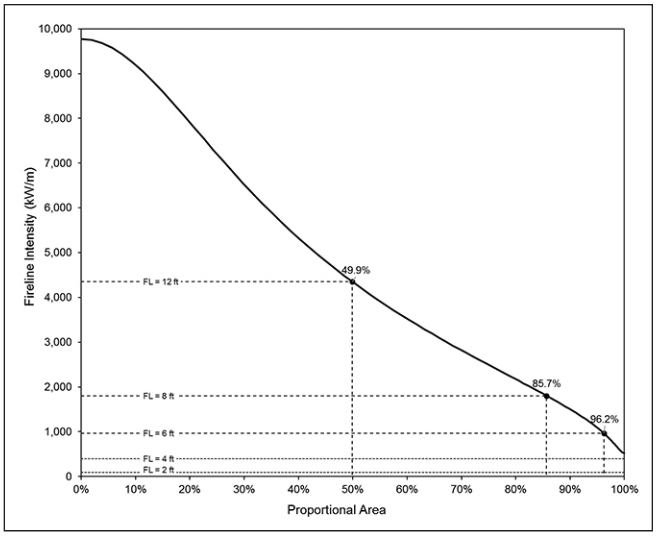

Figure 3—For a surface headfire intensity of 9,770 kW/m at a 20-ft wind speed of 15 mi/h (*LB* = 2.275), one can find the proportional fire-area burned at the fireline intensities that correspond to class breaks in the FIL classification. Those proportional areas determine the flame-length exceedance probability for each FIL. Flame-length probability for a class is found by subtraction. For example, the probability of FIL5 (flame lengths between 8 and 12 ft) is 35.8 percent (85.7 percent to 49.9 percent).

Table 3—Seven weather types defined only by 20-ft wind speed. Temporal relative frequency is a measure of how often these weather types occur. Relative burn-period length is a measure of the relative length of a daily burning period for each weather type.

Weather type (w)	20-ft wind speed (mi/h)	Temporal relative frequency % (TRF_w)	Relative burn-period length ($RBPL_w$)
1	0–1	6.2	1.0
2	1–5	20.2	1.2
3	5–10	58.9	1.4
4	10–15	13.1	1.6
5	15–20	1.0	1.8
6	20–25	0.5	2.0
7	25–30	0.1	2.2

WEIGHTING WEATHER TYPES

The above example illustrated that a given headfire intensity can be divided into the relative proportions of fire-area burned in predefined intensity classes for a single weather type—one wind speed, one wind direction, and one set of fuel moisture contents. Such weather types can be classified in a variety of ways but are typically organized by binning wind speed and wind direction, and by establishing one or more fuel moisture scenarios. Fire planning applications should ideally account for the full range of weather types that can occur, not just the most common or most extreme types.

To illustrate the weighting of multiple weather types, the single fuel moisture scenario described above will be extended to accommodate a full range of wind speeds. Wind direction is irrelevant in this example because flat ground was assumed, so there is no wind-slope alignment to consider. RAWS data for sustained 20-ft wind speed for the month of August (noon to 8 p.m. local time) were summarized to find the relative frequency distribution of wind speed as shown in table 3.

A time-weighted mean flame-length probability would be an improvement over using only a single weather condition to find flame-length probabilities, but it fails to account for drastically different potentials for burned area among the weather types. Lower fuel moisture and, especially, higher wind speeds, lead to greater spread rates. Higher spread rates in turn result in exponentially greater burned area. Daily burn-period length (hours of spread per day) may be longer for certain weather types (low moisture content and/or high wind, for example). If weather types had equal temporal probabilities of occurring, the higher wind speeds would account for a disproportionately large share of total area burned.

The solution presented here is to calculate a new area-based weighting factor that accounts for both the temporal relative frequency of a weather type and the relative contribution of that weather type to overall area burned, based on the rate of spread, relative burn-period length, and the dimensions of an ellipse. The basic area-weighted mean calculation is similar to that for time weighting but requires a new area-weighted relative frequency for each weather type (ARF_w). For example, the area-weighted conditional probability of fire in *FLP*1 is:

$$FLP1 = \sum FLP1_w * ARF_w$$

where $FLP1_w$ is the flame-length probability for weather type w and FIL1, and ARF_w is the area-weighted relative frequency of weather type w. ARF_w is calculated by combining TRF_w with an area-burned index (ABI_w):

$$ARF_w = \frac{TRF_w * ABI_w}{\sum(TRF_w * ABI_w)}$$

where TRF_w is the temporal relative frequency of weather type w. ABI_w is assumed to be proportional to the area of an ellipse:

$$ABI_w \propto \pi abt^2$$

where t is a variable representing the length of time of fire spread. Substituting a/LB for b, omitting the constant π, which does not affect the *ARF* weighting, and substituting for t a variable representing the relative burn-period length (minutes or hours per burn day; $RBPL_w$), *ABI* simplifies to:

$$ABI = \frac{a^2 * RBPL^2}{LB}$$

The *RBPL* factor will not play a role in the calculation unless it is allowed to vary among the different weather types. For example, drier and windier weather types may be associated with a longer daily burning period. ABI_w is therefore a function of the overall length of the ellipse and the *LB* ratio. The overall elliptical length can be estimated from the headfire *ROS*, *BR*, and *RBPL*. For this example, *RBPL* was assumed to increase with wind speed (table 3).

First, headfire *ROS* and *FLI* are calculated for the various weather types; from those results ABI_w and ARF_w are calculated using the equations above (table 4). Note that, compared to the *TRF* weighting factors, the *ARF* weighting factors give higher weight to the higher wind speed weather types and lower weight to the lower wind speed types. This is due to higher spread rates for higher wind speeds and the assumed longer *RBPL* for higher wind speeds, both of which increase *ABI*.

Next, the *FLP* calculations were done for each weather type independently, and the ARF_w factors from table 4 were used to calculate the overall weighted-mean *FLP*s (table 5). A graphical comparison of the *FLP*s resulting from the *TRF* and *ARF* weighting schemes illustrates the shift toward higher intensities when using the *ARF* weighting factors (fig. 4).

APPLICATIONS OF FLEP-GEN

FLEP-Gen is a process by which flame-length probabilities are deterministically generated for a given fuel complex (surface and canopy fuel characteristics) and set of weather conditions. The examples in this paper are inherently nonspatial—one point on the landscape. However, the FLEP-Gen process can be implemented spatially using custom applications of available fire-behavior modeling systems.

FLEP-Gen has many potential applications in wildfire incident and fuel management planning. Hazard and risk assessments are now being generated for individual wildfire incidents in order to better assess a wildfire's potential fire effects on resources and assets (Hollingsworth and Panunto 2017), enabling improved allocation of firefighting resources among competing wildfires. During a wildfire incident, the current and foreseeable weather conditions may be different than those used with a stochastic simulator based on long-term historical weather data covering entire fire seasons. Currently available deterministic methods can be based on incident-specific weather conditions (Hollingsworth and Panunto 2017) but still suffer from their focus on the head of a fire and a single weather condition, which can lead to overprediction of fire intensity and subsequent mischaracterization of fire effects. The FLEP-Gen process can be run with any set of weather types, including incident-specific conditions.

Assessing wildfire hazard consists of two components—wildfire likelihood and wildfire intensity given that a fire occurs. The wildfire intensity component is often estimated with a single flame-length value, usually for a given percentile weather condition, such as the 90th percentile. Flame length is typically estimated for the head of the fire for that weather condition. The FLEP-Gen process improves the estimation of wildfire intensity for a hazard assessment by incorporating non-heading spread directions, which produce lower intensities than at the head, and can incorporate a variety of wind speeds, wind directions, and moisture content scenarios.

Table 4—The temporal relative frequency, headfire behavior characteristics, area-burned index, and Area-based relative frequency for seven weather types (as defined by wind speed).

Weather type (w)	Temporal relative frequency (TRF_w) %	Headfire intensity (kW/m)	Headfire spread rate (m/min)	Headfire flame length (ft)	Area burned index (ABI_w)	Area-based relative frequency (ARF_w) %
1	6.2	590	1.89	4.8	2.068	0.1
2	20.2	2,798	8.95	9.8	34.93	5.1
3	58.9	6,113	19.6	14.0	137.4	58.6
4	13.1	9,770	31.3	17.4	305.0	28.9
5	1.0	13,668	43.7	20.3	522.7	3.8
6	0.5	17,757	56.8	22.9	768.9	2.8
7	0.1	22,004	70.4	25.3	1,019.5	0.7

Table 5—Flame-length probabilities for the six standard fire intensity levels (FILs), along with the time-weighted mean and area-weighted mean flame-length probabilities. FIL1 = 0–2 ft flame length; FIL2 = 2–4 ft; FIL3 = 4–6 ft; FIL4 = 6–8 ft; FIL5 = 8–12 ft; and FIL6 = 12+ ft.

Weather type	FIL1 %	FIL2 %	FIL3 %	FIL4 %	FIL5 %	FIL6 %
1	0.0	0.0	100.0	00.0	00.0	00.0
2	0.0	0.0	15.2	31.7	53.1	00.0
3	0.0	0.0	00.6	09.7	33.6	56.1
4	0.0	0.0	03.8	10.5	35.8	49.9
5	0.0	0.0	03.2	09.9	33.8	52.9
6	0.0	0.2	03.3	10.9	34.0	51.4
7	0.0	0.2	04.1	13.0	34.8	47.6
Weighted mean	**0.0**	**0.0**	**02.6**	**11.1**	**35.3**	**51.1**

Wildfire hazard, as defined above, is the foundation of an effects analysis. An effects analysis represents the full implementation of the wildfire risk assessment framework (Scott et al. 2013). An effects analysis relies heavily on an estimate of *FLP*s across the landscape. Presently, the estimate of *FLP*s for an effects analysis is limited by one or more factors:

- spatial resolution (cell size) of the stochastic simulation used to generate the *FLP*s;
- small sample size per grid cell from a stochastic simulator;
- limited weather conditions for a deterministic simulation; and
- headfire-only for a deterministic simulation.

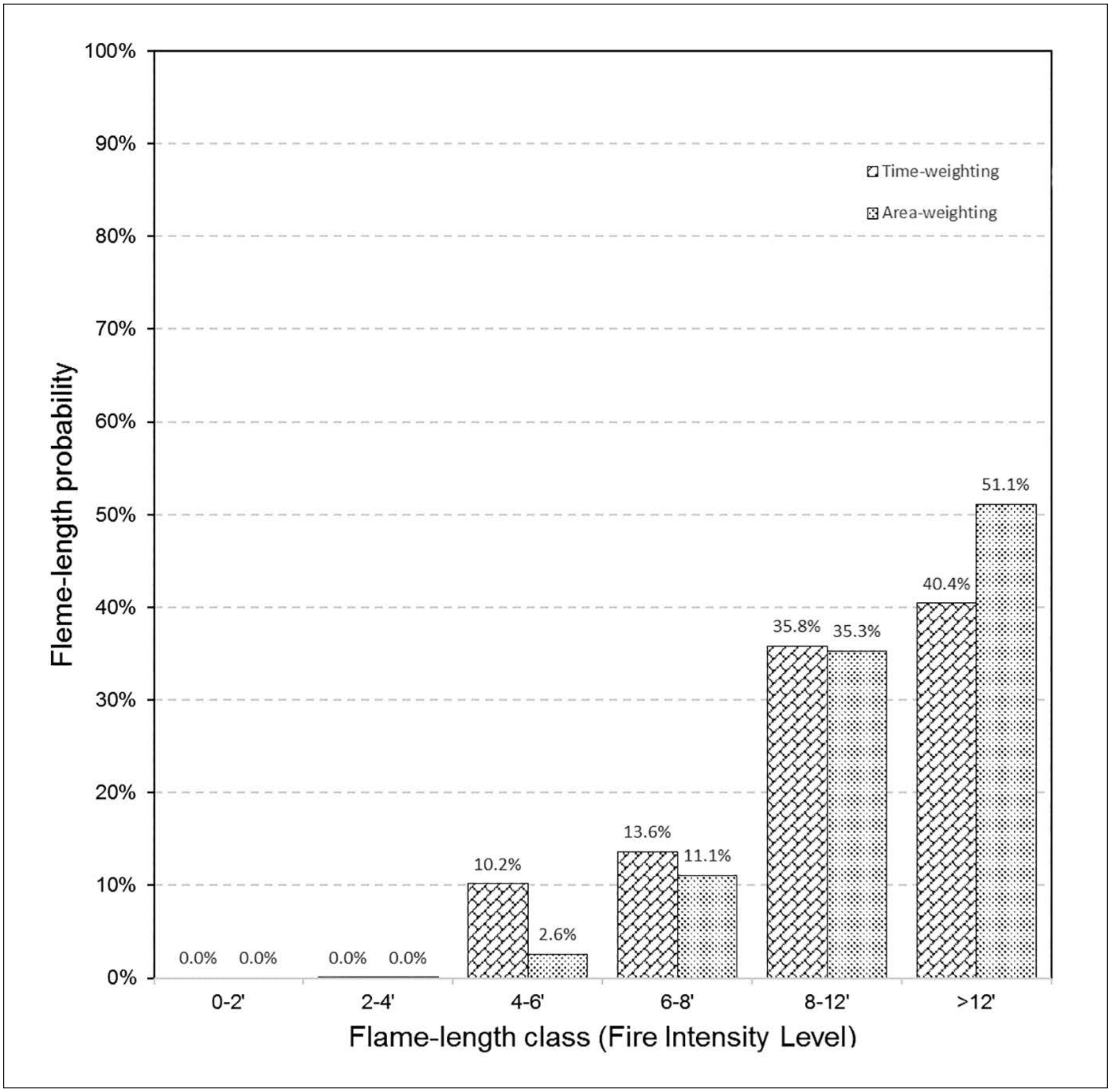

Figure 4—Comparison of integrated flame-length probabilities resulting from simple time-weighting (slanted bricks) of multiple wind speeds and area weighting (fine dots). If no consideration were given to non-heading intensity or to weighting multiple weather scenarios, fire intensity would be in the > 12-ft FIL with 74 percent probability (time weighting) or 95 percent (area weighting), because the headfire flame length exceeds 12 ft for all but the mildest weather types.

The FLEP-Gen process may be able to generate flame-length probability rasters suitable for an effects analysis at finer resolutions than is possible with a stochastic simulator and does not suffer from a problem of small sample size where BP is low. Instead, the FLEP-Gen process integrates flame-length probabilities for all possible weather scenarios, not only those that burned a given pixel, which may be biased toward extreme conditions in areas of lower burn probability. The process improves upon prior uses of deterministic simulations in an effects analysis by correctly weighting weather types and by incorporating fire intensity in non-heading spread directions.

The deterministic nature of the FLEP-Gen process makes it well suited to fuel management planning applications. It is relatively straightforward to generate an "ideal" fuelscape as a companion to the current-condition fuelscape. The ideal fuelscape represents the ideal treated fuel condition, without specific consideration to exactly how the ideal condition is attained (some combination of mechanical treatment and prescribed fire is assumed). For the ideal fuelscape, one can generate another set of *FLP*s, then compare those *FLP*s with the current condition to see how intensities are affected by the treatment.

Even better, the current the current condition and ideal fuelscapes can be used in the effects analysis to generate two *cNVC* rasters. This will show not only where the flame length is reduced, but it also emphasizes that it is much more desirable to reduce flame lengths in some parts of the landscape than others. The difference in *cNVC* rasters is an indication of the effects of the treatment on reducing wildfire risk to resources and assets.

The risk-reduction potential can then be summarized for any number of summary zones—by stand, hydrologic unit, admin unit (Region/Forest/District), political unit (city/county/State), fire district, etc. The summaries can then be used to support fuel management funding decisions and prioritization.

Finally, the FLEP-Gen process can be used in a measure of fuel management program performance. The FLEP-Gen process can be conducted for the current condition and for the proposed or actual posttreatment fuel condition. After running through an effects analysis, the total amount of risk-reduction accomplished by the treatment can be estimated and used to measure performance.

DISCUSSION

The FLEP-Gen process produces a set of *FLP* rasters comparable to those produced by a stochastic simulator. FLEP-Gen improves upon currently available deterministic methods by accounting for non-heading spread and integrating multiple weather scenarios. Though the example used the six-bin fireline intensity classification employed by FSim, the process can be adapted to fit with any desired fireline intensity classification.

FLEP-Gen is not computationally limited, as with stochastic simulators like FSim, to a coarser resolution for larger landscapes. It can be run at a 30-m pixel size consistent with native LANDFIRE data. Additionally, the FLEP-Gen results cover all possible weather scenarios input to the calculations and are not subject to the problem of small sample sizes associated with stochastic modeling, whereby pixels burn as few as 10 times in a 10,000-season simulation.

For this paper, results were based on a single set of fuel moisture inputs representing the 97th percentile weather and flat ground (which obviates wind direction). The process allows wind speed, wind direction, and fuel moisture to co-vary according to their distributions in the historical weather record. Further, an analyst can enable fuel moisture conditioning in FlamMap to allow fuel moistures to vary according to the environmental and topographic characteristics associated with each pixel. This feature is available in the current set of deterministic models but most commonly used in conjunction with a single wind speed and direction and heading intensities. This feature is not presently available in stochastic simulation models. Finally, an analyst can enable WindNinja (Forthofer et al. 2009) to downscale and vary wind patterns spatially across the landscape and integrate those results with the non-heading spread and multiple wind speeds used by the FLEP-Gen.

FLEP-Gen results and the associated cNVC grid(s) can be combined with burn probability grids produced by another tool such as FSim, RANDIG, or FSPro to generate an expected net value change raster (eNVC).

This information could be used in fuel treatment prioritization to evaluate where fuel treatments can simultaneously produce the greatest reduction in risk to highly valued resources and assets, and where treatments are most likely to interact with fire on the landscape based on higher burn probability values. Using the perimeter event set, produced by the above stochastic models, to overlay with cNVC results from FLEP-Gen and calculate exceedance probability curves is likely to be of interest in incident-level risk assessment and for fire management decisionmaking across many ongoing incidents.

There are two main limitations of the FLEP-Gen process compared to stochastic simulation of *FLP*s. First, FLEP-Gen does not capture any effects of landscape or fire-weather heterogeneity (and resulting fire-spread topology) on fire intensity. For example, assuming there is a strong directional component to the wind, lee sides of nonburnable or slow-burning features can produce lower fire intensities in a stochastic simulator, because fires must flank or back through the area rather than spread as a headfire. Similarly, a wildfire on which the wind direction shifts drastically can result in a different proportion of heading behavior than would be estimated for a point-source fire. The FLEP-Gen process does not capture these phenomena.

Second, FLEP-Gen does not capture any effect of progressive fireline containment on overall fireline intensity. In FSim, if the perimeter-trimming function is enabled, fire perimeter is extinguished on the lowest-intensity portions of the perimeter first. Again, FLEP-Gen does not capture that phenomenon. However, initial testing of both factors shows them to be relatively small. Further testing of FLEP-Gen is underway.

ACKNOWLEDGMENTS

I am grateful to Dr. Elizabeth Reinhardt, Assistant Director, Fire and Aviation Management, Forest Service, U.S. Department of Agriculture (retired), for funding the initial development of this process; and to Rick Stratton, National Fire Analyst for Planning and Budget, Fire, and Aviation Management, for its ongoing development. The spatial wildfire analysts at Pyrologix (Julie Gilbertson-Day, Kevin C. Vogler, and April M. Brough) developed the spatial implementation of this process. I wish to thank Dr. Mark Finney (Research Forester, Forest Service, Rocky Mountain Research Station, Missoula Fire Sciences Laboratory) and Dr. Matthew Thompson (Research Forester, Forest Service, Rocky Mountain Research Station, Human Dimensions Project) for their helpful reviews of this paper.

REFERENCES

Albini, F.A.; Baughman, R.G. 1979. Estimating windspeeds for predicting wildland fire behavior. Res. Pap. INT-221. Ogden, Utah: U.S. Department of Agriculture, Forest Service, Intermountain Forest and Range Experiment Station. 12 p.

Alexander, M.E. 1982. Calculating and interpreting forest fire intensities. Canadian Journal of Botany. 60(4): 349–357.

Alexander, M.E. 1985. Estimating the length-to-breadth ratio of elliptical forest fire patterns. Proc. 8th Conf. Fire and Forest Meteorology: 287–304.

Byram, G.M. 1959. Combustion of forest fuels. In: Forest fire: Control and use, 2nd edition. New York, NY: McGraw-Hill.

Catchpole, E.A.; Alexander, M.E.; Gill, A.M. 1992. Elliptical-fire perimeter-and area-intensity distributions. Canadian Journal of Forest Research. 22(7): 968–972.

Finney, M.A. 1998. FARSITE: Fire Area Simulator—model development and evaluation. Res. Pap. RMRS-RP-4. Ft. Collins, CO: U.S. Department of Agriculture, Forest Service, Rocky Mountain Research Station. 47 p.

Finney, M.A. 2005. The challenge of quantitative risk analysis for wildland fire. Forest Ecology and Management. 211(1): 97–108.

Forthofer, J.; Shannon, K.; Butler, B. 2009. Simulating diurnally driven slope winds with WindNinja. In: Proceedings of 8th Symposium on Fire and Forest Meteorological Society. Kalispell, MT: American Meteorological Society.

Hollingsworth, L.; Panunto, M. 2017. Wildfire risk assessment for the Frye Fire. Unpublished Report to the Coronado National Forest.

Roose, H.; Ballard, L.; Manley, J.; Saleen, N.; Harbert, S. 2008. Fire program analysis system—preparedness module. In: González-Cabán, A., tech. ed. Proceedings of the second international symposium on fire economics, planning, and policy: a global view. Gen. Tech. Rep. PSW-GTR-208. Albany, CA: U.S. Department of Agriculture, Forest Service, Pacific Southwest Research Station: 377–384.

Scott, J.H. 2007. Nomographs for estimating surface fire behavior characteristics without a computer. Gen. Tech. Rep. RMRS-GTR-192. Fort Collins, CO: U.S. Department of Agriculture, Forest Service, Rocky Mountain Research Station. 119 p.

Scott, J.H. 2012. Introduction to wildfire behavior modeling. National Interagency Fuels, Fire, & Vegetation Technology Transfer. Available: http://pyrologix.com/wp-content/uploads/2014/04/Scott_20121.pdf.

Scott, J.H.; Thompson, M.P.; Calkin, D.E. 2013. A wildfire risk assessment framework for land and resource management. In: Gen. Tech. Rep. RMRS-GTR-315. U.S. Department of Agriculture, Forest Service, Rocky Mountain Research Station.

Thomas, P.H. 1963. The size of flames from natural fires. Proceedings of the Ninth International Symposium on Combustion. New York: Academic Press.

Thompson, M.P., Scott, J.; Helmbrecht, D.; Calkin, D.E. 2013. Integrated wildfire risk assessment: framework development and application on the Lewis and Clark National Forest in Montana. Integrated Environmental Assessment and Management. 9(2): 329–342.